Pattern of 4-Thiouridine-Induced Cross-Linking in 16S Ribosomal RNA in the *Escherichia coli* 30S Subunit†

Kavita Nanda and Paul Wollenzien*

Department of Molecular and Structural Biochemistry, North Carolina State University, Raleigh, North Carolina 27695-7622

Received February 10, 2004; Revised Manuscript Received May 7, 2004

ABSTRACT: The locations of RNA−RNA cross-links in 16S rRNA were determined after in vivo incorporation of 4-thiouridine (s^4U) into RNA in a strain of *Escherichia coli* deficient in pyrimidine synthesis and irradiation at >320 nm. This was done as an effort to find RNA cross-links different from UVB-induced cross-links that would be valuable for monitoring the 30S subunit in functional complexes. Cross-linked 16S rRNA was separated on the basis of loop size, and cross-linking sites were identified by reverse transcription, RNase H cleavage, and RNA sequencing. A limited number of RNA−RNA cross-links in nine regions were observed. In five regions—$s^4U562 \times C879-U884$, $s^4U793 \times A1519$, $s^4U1189 \times U1060-G1064$, $s^4U1183 \times A1092$, and $s^4U991 \times C1210-U1212$—the s^4U-induced cross-links are similar to UVB-induced cross-links observed previously. In four other regions—$s^4U960 \times A1225$, $s^4U820 \times G570$, $s^4U367 \times A55-U56$, and $s^4U239 \times A120$—the s^4U-induced cross-links are different from UVB-induced cross-links. The pattern of cross-linking is not limited by the distribution of s^4U, because there are at least 112 s^4U substitution sites in the 16S rRNA. The relatively small number of s^4U-mediated cross-links is probably determined by the organization of the RNA in the 30S subunit, which allows RNA conformational flexibility needed for cross-link formation in just a limited region.

The high-resolution ribosome structures determined by crystallography and cryo-EM[1] (*1*−*7*) have allowed a leap in the understanding of their mechanistic role in protein synthesis. However, it is still difficult to analyze complexes that represent the range of conformational states that probably occur in the ribosome during many of its reactions, and in addition, it is valuable to be able to obtain information about the ribosome conformations under physiological conditions. Intramolecular RNA−RNA interactions have been studied by a number of biochemical techniques, and UVB-induced photo-cross-linking is attractive because it can be carried out on native, highly active ribosomes without addition of chemical probes and, in principle, can be performed very rapidly. UVB irradiation with a transilluminator produces about 14 long-range intramolecular cross-links in *E. coli* 16S rRNA depending on the buffer conditions, temperature, and wavelength of irradiation (*8*, *9*). Under standard irradiation conditions, changes in cross-linking frequency are an indication of structural changes in the ribosomal RNA (*10*, *11*). Nanosecond UV pulse laser irradiation, used at intensities of $(4.5-18) \times 10^9$ W m^{-2}, results in the formation of four additional long-range RNA−RNA cross-links (as well as the cross-links seen with the low-intensity transilluminator) and increases the RNA cross-linking frequency (*12*). However, the use of laser intensities above 18×10^9 W m^{-2}, for instance, obtained in a picosecond pulse laser, is not a viable approach to seek additional RNA−RNA cross-links, because RNA strand breakage is proportional to the intensity.

An alternative RNA cross-linking method that could have greater efficiency and a pattern different from that of UVB cross-linking under both in vitro and in vivo conditions, with minimal side reactions, is UVA irradiation of 4-thiouridine (s^4U)-containing RNA (*13*−*16*). The presence of s^4U results in minimal perturbations of the polynucleotide chains into which it is incorporated (*17*). The main π, π^* absorption band of uracil is shifted from 260 to 330 nm, allowing irradiation at 330−350 nm to efficiently convert it to a highly reactive species that forms stable, covalent bonds within a limited distance (*13*). In several instances where UVB and UVA/s^4U cross-linking of RNA to proteins were compared, a larger number of RNA−protein cross-links were found with the UVA/s^4U samples (*14*−*16*). s^4U has also been used to induce RNA−RNA cross-linking. Long-range RNA−RNA cross-links (cross-link between nucleotides distant in the primary sequence) have been identified in fragments of thiolated 16S rRNA prepared by in vitro transcription (*18*), or in complete 16S rRNA with s^4U at specific positions, reconstituted to 30S subunits (*19*). s^4U forms Pyo(4−5)Pyr- and Pyo(4−6)Pyr-type (*20*−*21*) adducts with pyrimidines, and photoadducts between 4-thiothymidine and adenosine also form by a (2 + 2) cycloaddition to the N7/C8 double

† This work was supported by National Institutes of Health Grant GM 43237 to P.W.

* To whom correspondence should be addressed. Phone: (919) 515-5703. Fax: (919) 515-2047. E-mail: paul_wollenzien@ncsu.edu.

[1] Abbreviations: s^4U, 4-thiouridine; β-ME, β-mercaptoethanol; bis-Tris, [bis(2-hydroxyethyl)amino]tris(hydroxymethyl)methane; EDTA, ethylenediaminetetraacetic acid; Phe-tRNA^{Phe}, phenylalanyl-tRNA^{Phe}; poly(U), polyuridine mRNA; rRNA, ribosomal RNA; Tris, tris(hydroxymethyl)aminomethane; TBE, Tris, borate, EDTA; BTBE, bis-Tris, borate, EDTA; APM, (*N*-acrylylaminophenyl)mercuric chloride; APAB, azidophenacyl bromide; PAGE, polyacrylamide gel electrophoresis; cryo-EM, cryo electron microscopy, $T_{20}A_{200}M_{20}$ β_{10}, 20 mM Tris−HCl, pH 7.4, 200 mM NH_4Cl, 20 mM $MgCl_2$, 10 mM β-ME; $T_{20}A_{200}M_3$ β_{10}, 20 mM Tris−HCl, pH 7.4, 200 mM NH_4Cl, 3 mM $MgCl_2$, 10 mM β-ME.

10.1021/bi049702h CCC: $27.50
Published on Web 06/25/2004

bond of adenosine (*22*). In fact, in the s^4U RNA cross-linking experiments, cross-links involving s^4U and both pyrimidines and purines have been found (*18*, *19*).

A strategy for in vivo incorporation of s^4U into ribosomes has been described by the Favre group (*24*, *25*), using a *PyrD* mutant strain of *E. coli*. The *pyrD*$^-$ strain is unable to synthesize pyrimidine bases and is dependent on an external uridine source. The strain is viable on a mixture of uridine and s^4U, and the amount of s^4U incorporated into high molecular weight RNA in the cell depends on the uridine to s^4U ratio and the growth conditions of the cell culture. The present work optimized the incorporation of s^4U to obtain a reproducible pattern of RNA−RNA cross-links in the 16S rRNA, which should be less than one per 16S rRNA, and to obtain a good yield of active ribosomes. Methods that systematically identify long-range cross-links in the 16S rRNA were used to isolate and determine RNA cross-linking sites.

MATERIALS AND METHODS

Strain and Growth Media. Strain AB1157 is an *E. coli* K12 *F- Leu, Pro, His, Arg, Thr, Gal, Xyl, Man, Lac*. The strain used is a derivative of AB1157 carrying *SfiA* and *PyrD* mutations. It is a gift from Dr. Richard D'Ari, Institute Jacques Monod, University of Paris. The preculture growth medium was 63 B1: 0.1 M KH_2PO_4, 15 mM $(NH_4)_2SO_4$, and $FeSO_4$ (0.005 mg/L) with pH adjusted to 7.0 using KOH (*25*), complemented with a final concentration of 0.2% glucose, 0.4% casamino acids, 40 μg/mL uridine, 1 mM $MgSO_4$, and 1 μg/mL vitamin B1 and containing 50 μg/mL kanamycin. This will be referenced below as "63 B1 complemented and with kanamycin".

It has been seen previously that, at an s^4U/U ratio of 2.5 and temperature of 30 °C, the growth of the mutant strain is linear with efficient s^4U incorporation in 70S (*23*). 4-Thiouridine uptake into RNA was also dependent upon the age of the preculture, i.e., the number of generations the cells have undergone immediately before dilution in the thiolation medium (*24*). At $2.5 < N < 4$, the cells grew exponentially with significant incorporation of s^4U, and at $N = 3$, the yield of stable 70S ribosomes (defined operationally as the fraction of associated 70S which were separated from unassociated 30S and 50S in $T_{20}A_{200}M_{20}\,\beta_{10}$) was 55% with ~70−75 s^4U residues per 70S.

In the present study, an overnight preculture of AB1157 grown at 30 °C in 63 B1 complemented and with kanamycin was added to the same medium at a concentration of $A_{650} = 0.00625$. This was grown to $A_{650} = 0.05$. 4-Thiouridine was then added to the medium, and the cells were grown until A_{650} was 0.5. The final concentration of s^4U used in the thiolation medium was 75 μg/mL to give an s^4U/U ratio of about 2. Cells were then pelleted and processed immediately for ribosome purification. These conditions resulted in an incorporation of s^4U that gave a reproducible and well-defined pattern of cross-linking as judged by denaturing polyacrylamide gel electrophoresis.

Ribosome Preparation and Cross-Linking. Ribosomes were extracted from the cells as described before (*26*). All operations were performed at 4 °C. 70S ribosomes were separated from nonassociated 50S and 30S subunits in 10−40% linear sucrose gradients prepared in $T_{20}A_{200}M_{20}\,\beta_{10}$ buffer by centrifugation in a SW 28 rotor at 18000 rpm for 18 h. 30S ribosomal subunits were prepared from 70S ribosomes by incubating them for 3 min at 37 °C in $T_{20}A_{200}M_3\,\beta_{10}$, followed by centrifugation on 10−40% linear sucrose gradients, prepared in the same buffer, at 27000 rpm for 18 h in the SW 28 rotor. 30S subunits were collected, adjusted to 20 mM Mg^{2+}, and concentrated by pelleting at 40000 rpm overnight in a Ti 50.2 rotor. The 30S subunits were dissolved in $T_{20}A_{200}M_{20}\,\beta_{10}$ buffer, aliquotted, and stored in −80 °C.

Activation of 30S subunits was done in $T_{20}A_{200}M_{20}\,\beta_{10}$ buffer for 15 min at 37 °C. Samples (usually 100 pmol of 30S subunits in 0.15 mL of $T_{20}A_{200}M_{20}\,\beta_{10}$ for a preparative-scale experiment or 10 pmol of 30S subunits in 0.05 mL of $T_{20}A_{200}M_{20}\,\beta_{10}$ for an analytical experiment) in 1.5 mL polyethylene microfuge tubes were placed in a sample well, surrounded by a circulating 4 °C solution of $Co(NO_3)_2$ to remove light of <320 nm and to keep the sample cool. Irradiation was with two 400 W low-pressure Hg lamps for 10 min (*27*). Samples were treated with proteinase K, phenol and ether extracted, and ethanol precipitated. The RNA was dephosphorylated with shrimp alkaline phosphatase (USB, Cleveland, OH), phenol and ether extracted, and ethanol precipitated. 16S rRNA was purified on 1% agarose gel and 5′-end-labeled with [γ-^{32}P]ATP by T4 polynucleotide kinase (MBI Fermentas, Hanover, MD) or 3′-end-labeled with [5′-^{32}P]pCp by T4 RNA ligase (*28*) as required by the experiment. For analytical evaluation of cross-linking, RNA was electrophoresed on 8.3 M urea, 3.6% (w/v) polyacrylamide gel (acrylamide:bisacrylamide = 40:1, w/w) in BTBE buffer as described (*8*).

For preparative separation of cross-linked RNA, approximately 30 μg of the cross-linked RNA was separated on a 10 cm wide well using the 3.6% (w/v) polyacrylamide gel. The location of the bands containing un-cross-linked and cross-linked 16S rRNA was determined with a PhosphorImager (Amersham, Piscataway, NJ). The bands were cut out of the gel and eluted by ultracentrifugation through cushions containing 2 M CsCl and 0.2 M EDTA, pH 7.4, for 12 h at 40000 rpm (*29*). RNA samples were redissolved in 250 μL of water, phenol and ether extracted, and precipitated at −20 °C. Samples were then dissolved in 10 μL of water except the linear RNA, which was dissolved in 50 μL of water.

Determination of Cross-Linked Sites. Reverse transcription analysis of 16S rRNA was performed as described before (*8*). Fifteen DNA primers complementary to different regions of 16S rRNA were used to read the whole molecule of 16S rRNA. Reverse transcription reactions were electrophoresed on 8% acrylamide/bisacrylamide (19:1), 8.3 M urea in TBE buffer. Cross-links were identified as the nucleotide one nucleotide 5′ to the reverse transcription stop.

RNase H reactions contained 20 pmol or less of [γ-^{32}P]-labeled RNA molecule and 50 pmol of oligonucleotide. The RNA was annealed with 50 pmol of DNA oligonucleotides or mixed oligonucleotides containing 2′-methylribo- and 2′-deoxyribonucleotides in annealing buffer (20 mM Tris−HCl, pH 7.8, 0.0635 mM NH_4Cl) in a total volume of 20 μL at 55 °C for 5 min (*30*). Two units of RNase H at a concentration of 2 units/μL in dilution buffer (20 mM Tris−HCl, pH 7.8, 50 mM KCl, 100 mM NaCl, 1 mM EDTA, 1 mM DTT, 50% glycerol) and 3 μL of 10 mM $Mg(OAc)_2$

were added to the annealed mixture, and the resulting mixture was kept at 55 °C for 10 min. A 5 μL sample of 10% SDS was added to stop the reaction. The samples were then analyzed by 3.6% polyacrylamide gel at a 19:1 ratio of acrylamide to bisacrylamide.

For isolation of RNA fragments after RNase H digestion, 100 pmol of cross-linked 16S rRNA was annealed with 250 pmol of oligonucleotide(s) in a 100 μL volume of annealing buffer and incubated at 55 °C for 5 min followed by addition of 15 μL of 10 mM $Mg(OAc)_2$ and 10 units of RNase H and an additional incubation at 55 °C for 10 min. For determination of the 1519 site, a DNA oligonucleotide complementary to the 16S rRNA interval 679−693 was used, and for the determination of the U793 site, an additional mixed oligonucleotide complementary to the 16S rRNA interval 749−763, $_mC_mA_mC_mC_mdTdGdAdG_mC_mG_mU_mC_mA_mG_mU$, was used. A 25 μL sample of 10% SDS was added to stop the reaction, and RNA was phenol and ether extracted before ethanol precipitation. The RNA fragments (679−1542 or 759−1542) were isolated on 1% agarose gels in TBE buffer. Purified fragments were 3′- or 5′-labeled as described above. Cross-linked RNA was separated by electrophoresis on denaturing 5% polyacrylamide gels (40:1 acrylamide/bisacrylamide), and bands containing linear RNA and cross-linked RNA were isolated as described above.

Alkaline hydrolysis was performed as described previously (*27*). 3′- or 5′-end-labeled RNA (∼1000 cpm) was incubated in hydrolysis buffer (25 mM Na_2CO_3, pH 9.0, 0.5 mM EDTA) at 90 °C for 8 min, and RNase T1 sequencing was performed on control and cross-linked RNA samples (*28*). All samples were immediately cooled to 0 °C and analyzed on 10% polyacrylamide gel at a 19:1 ratio of acrylamide to bisacrylamide.

Determination of Cross-Linking Frequencies. 16S rRNA was obtained from the cross-linked 30S subunits as described before and resolved by electrophoresis on denaturing 3.6% polyacrylamide (40:1 acrylamide/bisacrylamide) gel containing 0.003% APM (*31*). A series of bands of reduced mobility were seen in addition to the band that has the mobility of native nonthiolated 16S rRNA. RNA from the topmost band, which has the maximum number of s^4U's, and RNA from intermediate bands, which has an apparent number of 4−6 s^4U's, were purified from the gel slices by centrifugation through cushions containing 2 M CsCl, 0.2 M EDTA, pH 7.4, 15 mM DTT for 12 h at 40 000 rpm (*29*). The RNA samples were re-electrophoresed on denaturing 3.6% polyacrylamide (40:1 acrylamide/bisacrylamide) gel to determine the cross-linking frequency. The frequency of cross-linking was determined from PhosphoImager data (ImageQuant, Amersham, Piscataway, NJ). To normalize for RNA loading, the cross-link band intensity was referenced to the 16S rRNA parent band in the same lane.

Analysis of Locations of s^4U in 16S rRNA by APAB Reaction and Reverse Transcription. Nonirradiated s^4U-containing 16S rRNA was prepared from thiolated 30S subunits and resolved by electrophoresis on denaturing 3.6% polyacrylamide (40:1 acrylamide/bisacrylamide) gel containing 0.003% APM as described previously. RNA from eight bands and the nonthiolated band was purified from the gel slices by ultracentrifugation through CsCl solution as described (*28*) in the presence of 15 mM DTT to the solutions. The RNA fractions were resuspended in 5 mM DTT and ethanol precipitated. A 2 μg sample of RNA from each band was reacted with APAB as described before (*32*). RNA was dissolved in 98 μL of a buffer containing 50 μM DTT, 50 mM Tris−HCl, pH 8.0, and to this was added 2 μL of APAB (100 mM APAB dissolved in 100% methanol). The reaction mixture was incubated at room temperature for 1 h in the dark and ethanol precipitated. RNA samples were finally redissolved in 10 μL of H_2O and analyzed by reverse transcription assay in reduced lighting as described above.

Re-irradiation of Cross-Linked RNA. A 10 pmol sample of 30S subunits was activated and irradiated with wavelength >320 nm for 10 min at 5 °C, treated with proteinase K, phenol and ether extracted, and ethanol precipitated. 16S rRNA was purified on 1% agarose gel and 5′-end-labeled with [γ-^{32}P]ATP and polynucleotide kinase after phosphatase treatment. The RNA was redissolved in 50 μL of 1 mM Tris−HCl, pH 8.0, and reirradiated at 5 °C for different lengths of time at wavelengths of 254 and 330 nm to determine if any cross-links were photoreversible. Samples were ethanol precipitated and redissolved in H_2O and formamide for gel electrophoresis on the denaturing 3.6% polyacrylamide gel system.

RESULTS

Preparation and Characterization of 70S Ribosomes with s^4U. In vivo incorporation of s^4U in *E. coli* ribosomes was done as described before (*24*, *25*) using a derivative of *E. coli* strain AB1157, carrying a mutation in *pyrD* to allow s^4U incorporation. The strain is deficient in pyrimidine synthesis but is capable of growing when uridine is included in the medium. Conditions for growth of the cells and suitable incorporation of s^4U have been described previously (*24*, *25*).

For the present study, cells were grown at 30 °C in medium containing uridine at 40 μg/mL for three generations (about 2 h) followed by the addition of s^4U to a final concentration of 75 μg/mL and grown for an additional three generations (3−4 h) determined by A_{650} measurements. The fraction of ribosomes that were isolated as 70S particles after sucrose gradient centrifugation was found to be ∼60% of the total soluble ribosomes. The s^4U-containing 30S subunits used for subsequent experiments were obtained from those 70S ribosomes to ensure their functional competence. 16S rRNA obtained from these 30S subunits was found to have an average of eight s^4U's per 16S rRNA as determined by spectrometric analysis (*23*). This 16S rRNA was also analyzed for the level of substitution of s^4U by electrophoresis on denaturing 3.6% polyacrylamide (40:1 acrylamide/bisacrylamide) gel containing APM, which retards the RNA through mercury−sulfur interactions (*18*, *31*). Eight bands corresponding to different levels of s^4U substitution were seen; the top band should be the most highly substituted 16S rRNA molecules (Figure 1 in Supporting Information). About 60% of the 16S rRNA ran at the nonthiolated 16S rRNA position, implying either that some RNA escaped interaction with APM due to the location of the s^4U in the molecule (*24*) or that there was still a large pool of nonsubstituted ribosomes under the conditions the cells were grown. Of the 40% of the 16S rRNA that has reduced electrophoretic mobility on the APM−polyacrylamide gel, the largest amount was in the topmost band, indicating substitution with eight s^4U's or more, if there is a direct counting of the bands and the s^4U incorporation.

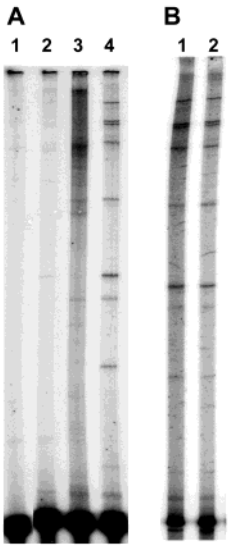

FIGURE 1: Gel electrophoresis analysis of s^4U-mediated RNA cross-linking. For all samples, 16S rRNA was first isolated on agarose gels and then 5′-[^{32}P]-labeled. Electrophoresis was done on 8.3 M urea, 3.6% polyacrylamide gels. (A) Lane 1, native (nonthiolated) 30S subunits irradiated with $\lambda \geq 320$ nm; lane 2, thiolated 30S subunits not irradiated; lane 3, thiolated deproteinated 16S rRNA irradiated with $\lambda \geq 320$ nm; lane 4, thiolated 30S subunits irradiated with $\lambda \geq 320$ nm. (B) Gel electrophoresis of cross-linked 16S rRNA after enrichment for s^4U content on APM gels: lane 1, thiolated 30S irradiated with $\lambda \geq 320$ nm and enriched for high substitution of s^4U per 16S rRNA; lane 2, thiolated 30S irradiated with $\lambda \geq 320$ nm and enriched for moderate substitution of s^4U per 16S rRNA.

The 30S subunits isolated from 70S ribosomes were tested for their activity in reassociation with 50S subunits and tRNA binding. Association of thiolated 30S with native 50S subunits, assayed by velocity sedimentation analysis on sucrose gradients in $T_{20}A_{200}M_{20}$ buffer, was identical to the behavior of nonsubstituted 30S subunits. $tRNA^{Phe}$ binding to poly(U)-programmed 70S ribosomes was determined by footprinting using the kethoxal reactivity at G926 as an index of tRNA binding (*33*−*35*), and similar levels of $tRNA^{Phe}$ binding were found in the s^4U-substituted and nonsubstituted samples (results not shown).

Dependence of RNA Cross-Linking on s^4U and Irradiation. Irradiation of nonthiolated and thiolated 30S subunits was done to determine the specificity of the cross-linking. The extent and pattern of cross-linking in the RNA, after 16S rRNA purification and 5′-[^{32}P]-labeling as described in the Materials and Methods, was determined by electrophoresis on denaturing 3.6% polyacrylamide gels at a 40:1 ratio of acrylamide to bisacrylamide (*8*). Cross-linked RNA molecules separate on the basis of loop size—the distance in the sequence between the nucleotides participating in the covalent cross-link (*8*, *18*, *19*, *36*). The occurrence of the RNA−RNA cross-links depended on both s^4U substitution and irradiation (Figure 1A). In addition, the pattern of cross-linking when 16S rRNA deproteinated before irradiation was very different from the pattern observed in the 30S subunit. In the deproteinated RNA a diffuse pattern of radioactive RNA was seen in the gel electrophoresis, indicating that a large number of cross-link products were produced, but none of them at a high frequency. In the 30S subunit, at least nine distinct bands were seen (Figure 1A).

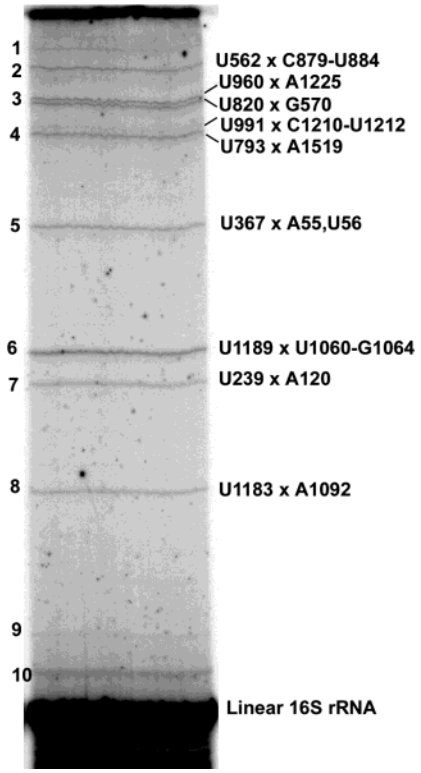

FIGURE 2: Preparative gel electrophoresis separation of cross-linked RNA. UV cross-linked 16S rRNA (not enriched for s^4U content) was electrophoresed on denaturing 3.6% polyacrylamide gel at a 40:1 ratio of acrylamide to bisacrylamide. Bands are numbered 1−10 on the left of the panel, and the cross-link identities, summarized from subsequent reverse transcription analysis and RNA sequencing, are written on the right of the panel. All the cross-links were identified except 1, 9, and 10. Linear 16S rRNA represents the un-cross-linked RNA.

Levels of s^4U substitution in the isolated 30S subunits are not random after three generations of growth with s^4U in the medium, so the pattern of cross-linking was determined after separation on APM−polyacrylamide gels to find out whether s^4U substitution levels affect the cross-linking pattern. After 10 min of irradiation in the 30S subunit, RNA was isolated, [^{32}P]-labeled, and purified on APM-containing polyacrylamide gels. The separation of the RNA in this case is likely due to residual s^4U remaining in the molecules even after the irradiation. 16S rRNA was isolated from regions of the gel that corresponded to ≥8 s^4U's per 16S rRNA or 4−6 s^4U's per 16S rRNA in unirradiated 16S rRNA, but because the original incorporation levels were not known, these will be referred to as highly- and moderately-s^4U-substituted 16S rRNA. The RNA was analyzed by gel electrophoresis on the 3.6% polyacrylamide gel. The frequency of the cross-linking is 2−3 times higher in the highly substituted 16S rRNA, but the pattern of cross-linking is not changed (Figure 1B).

Determination of Cross-Linking Sites. Ten bands as well as a strong band in the position of the unirradiated 16S rRNA were seen after gel electrophoresis of a RNA sample that came from cross-linking in 30S subunits (Figure 2). RNA from those regions of the gel was purified by centrifugation through CsCl solution (*29*). Each of the RNA fractions obtained from the gel was re-electrophoresed to check the separation of the cross-linked molecules (results not shown). All fractions were analyzed by reverse transcription, and

Table 1: Identity and Properties of s^4U Cross-Links in 30S Ribosomal Subunits

cross-link no.	identity	freq[a]	freq[a]	internucl dist[b] (Å)	similarity to UVB cross-link?[c]
2	U562 × C879	0.26	0.10	21.0	yes, [559−566]× [850−890] (a), U562 × U884 (b)
	U562 × C880	0.51	0.20	17.9	
	U562 × G881	0.53	0.21	15.1	
	U562 × C882	0.59	0.23	11.4	
	U562 × C883	0.62	0.24	7.3	
	U562 × U884	0.60	0.23	3.3	
3a	U960 × A1225	3.35	1.53	4.0	no
3b	U820 × G570	3.49	1.73	5.2	no
4a	U991 × C1210	0.12	nd	15.2	yes, U991 × U1212 (b)
	U991 × U1211	0.26	nd	12.7	
	U991 × U1212	0.34	nd	5.0	
4b	U793 × A1519	3.45	1.30	6.2	yes, U793 × A1518 (c)
5	U367 × A55	0.71	0.56	18.1	no
	U367 × U56	0.58	0.46	18.0	
6	U1189 × U1060	0.77	0.36	17.1	yes, [1065−1068] × [1188−1190] (a), G1064 × G1190 (d)
	U1189 × G1061	0.82	0.38	15.8	
	U1189 × U1062	0.72	0.34	14.2	
	U1189 × C1063	1.11	0.51	14.0	
	U1189 × G1064	0.73	0.34	13.9	
7	U239 × A120	0.76	0.40	5.3	no
8	U1183 × A1092	0.95	0.31	4.0	yes, A1093 × G1182 (b)

[a] Values for cross-link frequencies were taken from gel electrophoresis analysis. Frequencies are the percent of total RNA analyzed in each case. The first and second columns contain frequencies obtained with highly substituted 16S rRNA or moderately substituted 16S rRNA. Uncertainties are about 10% of the indicated values. nd = not determined. [b] Internucleotide distances were measured in the atomic structure of the 30S subunit obtained by X-ray diffraction (*2*). Distances were measured between the C4/S4 atoms of the uridine identified as the s^4U and the C5/C6 atoms of pyrimidine partners or N7/C8 atoms of purine partners. [c] UVB-induced cross-links were reported in (a) Stiege et al. (*47*), (b) Wilms et al. (*8*), (c) Shapkina et al. (*10*), and (d) Shapkina et al. (*12*). Cross-linking sites in brackets were determined by RNA fragmentation, which did not identify the precise nucleotide involved.

cross-linking sites were verified by analysis with oligonucleotide-directed RNase H cleavage.

Reverse transcription reactions using AMV reverse transcriptase and a set of 15 oligonucleotide primers were done to locate cross-linking sites. At cyclobutane-type cross-links such as those at the UV-induced cross-link between $tRNA^{Val}$ and 16S rRNA (*37*, *38*), at psoralen-induced cross-links (*39*), and at UV-induced cross-links in 16S rRNA made in the 30S subunit (*8*), AMV reverse transcriptase is stopped one nucleotide before the site of a cross-link, giving rise to a strong band in the primer extension pattern. s^4U-induced cross-links are also detected by reverse transcription (*18*, *19*), although a low-efficiency read-through at some cross-linking sites has been reported (*18*).

RNA from five bands (3a, 3b, 4, 7, and 8; see Figure 2) was found to have specific pairs of nucleotides as participants in the cross-links. This is similar to the situation seen in UVB-induced cross-linking. These five nucleotide pairs also have the property of small distances separating the reactive bonds in the 30S subunit structure as determined by measurements in the 16S rRNA tertiary structure in the 30S subunit (*2*) (see Table 1).

In four regions, series of reverse transcription stops were seen. In these cases, it was necessary to measure band intensities for all the stops to quantitatively evaluate the pattern. The positions having intensity at least 50% higher than that of the corresponding band in the control lane were taken as cross-linking sites. U562 was determined as the site of cross-linking in fraction 2 (Figure 3A), and the cross-linking partners were determined as C879, C880, G881, C882, C883, and U884 (Figure 3B). Similarly, U1189 was identified as the site of cross-linking in fraction 6 (Figure 3K), the cross-linking partners were U1060, G1061, U1062, C1063, and G1064 (Figure 3L), and U367 in fraction 5 (Figure 3G) was cross-linked to A55 and U56 (Figure 3H). Finally, a low-frequency band above band 4, which was resolved better at a 70:1 acrylamide:bisacrylamide ratio, was also found to have multiple cross-linking partners to a single nucleotide. It had U991 (Figure 3N) cross-linked to C1210, U1211, and U1212 (Figure 3O). In all four of these cases, a specific s^4U at one site forms cross-links with a series of partners from a limited interval of another part of the 16S rRNA.

For cross-link 3, which was not resolved very well on the gel system used here, four reverse transcription stops were seen (Figure 3). RNase H cleavage data (data not shown) and the mobility of the cross-links based on the loop size were used as criteria to assign the cross-links to each band. The band at the top (band 3a) was assigned to have a U960 × A1225 cross-link, and the band below (band 3b) was assigned the cross-link G570 × U820.

All of the cross-links were verified by oligonucleotide-directed RNase H cleavage. For verification of the cross-linked RNAs, DNA oligonucleotides complementary to the 16S rRNA on the 5′ side of the 5′-cross-linking site between the nucleotides involved in the cross-linking site and on the 3′ side of the 3′-cross-linking site were used. In the example shown for cross-link U1189 × G1064−U1060 (Figure 4B), the RNase H digestion was done with DNA oligonucleotides designated 1024, 1125, and 1264 corresponding to the intervals 1016−1032, 1117−1133, and 1256−1273, respectively. The oligonucleotides were annealed to the 3′-[^{32}P]-labeled 16S rRNA molecule containing the cross-link and digested with RNase H. The RNA was then analyzed on a

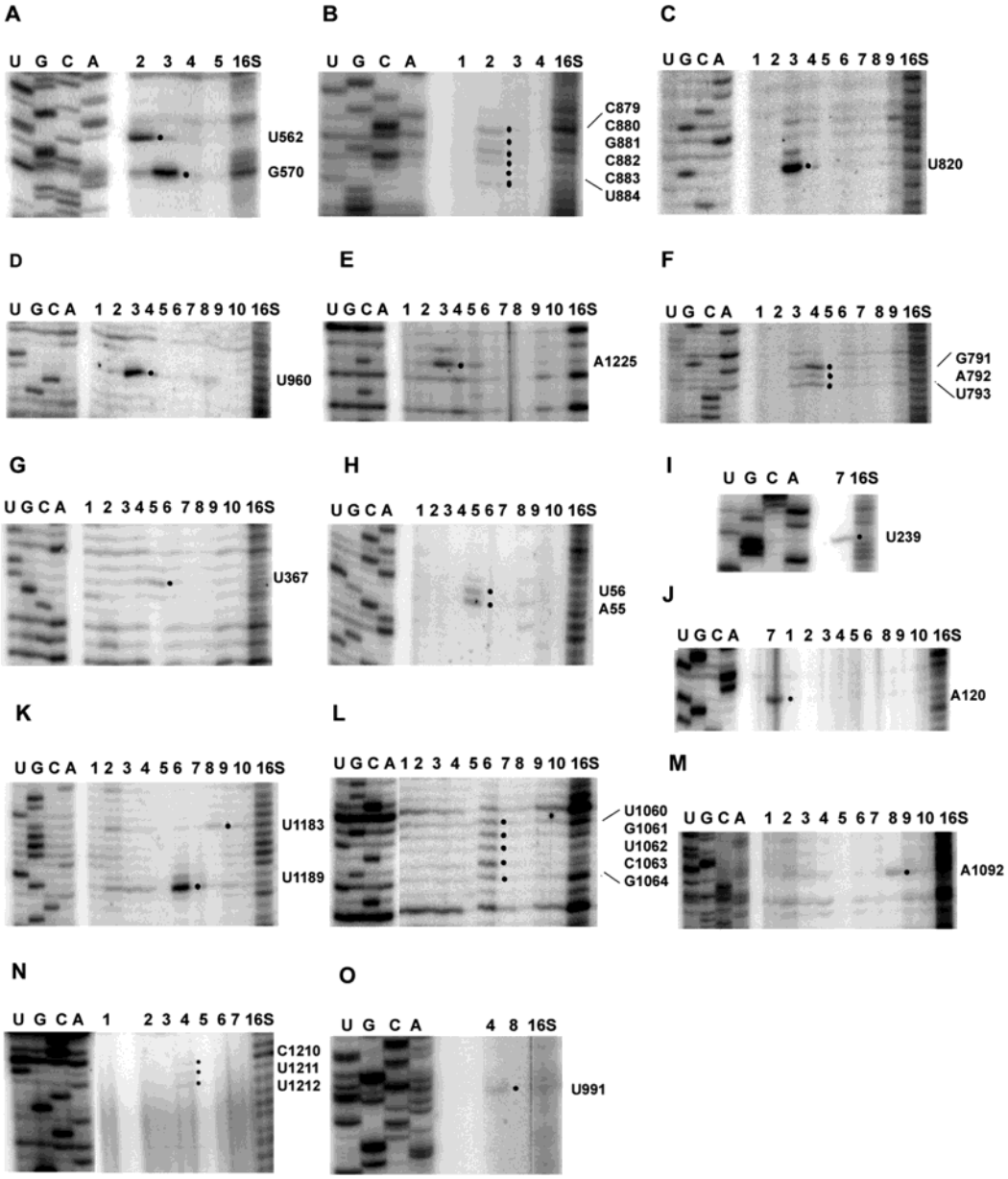

FIGURE 3: Reverse transcription analysis of cross-linked 16S rRNA substituted with 4-thiouridine, RNA from bands 1−10 and linear 16S from the preparative gel shown in Figure 2 were subjected to primer extension analysis using DNA primer complementary to 16S rRNA intervals at (A) 546−580, (B) 874−888, (C) 814−823, (D) 958−965, (E) 1224−1229, (F) 786−797, (G) 365−373, (H) 51−63, (I) 233−244, (J) 117−123, (K) 1180−1193, (L) 1057−1067, (M) 1080−1107, (N) 1209−1222, and (O) 979−1007. The right side of the panels indicates the cross-linked nucleotide number, one nucleotide on the 5′ side of the reverse transcription stop. Lanes U, G, C, and A are dideoxy sequencing lanes and indicate the nucleotide sequence of 16S rRNA.

denaturing 3.6% polyacrylamide gel at a 19:1 ratio of acrylamide to bisacrylamide. On the basis of the number and the size of the fragments, the approximate region of the cross-link was determined (Figure 4A). The fragment after RNase H cleavage with the 1264 oligonucleotide had mobility identical to that obtained from linear 16S rRNA (Figure 4A), implying that the region containing the cross-link was on the 5′ side of 1264 (Figure 4B). For a fragment produced by cutting with DNA oligonucleotide 1024, the RNA fragment had mobility slower than the RNA fragment obtained from linear 16S rRNA, implying that the cross-link was within the interval between 1024 and1542.

For the RNase H digestion with the oligonucleotide 1125, no fragmentation was seen. Since the same oligonucleotide was used as primer for the reverse transcription assay and since the RNA from fraction 6 did not inhibit RNase H, we conclude this oligonucleotide directed cutting in the middle of the cross-link loop, but the X-shaped product and the original looped molecule were not separated on the gel system used here. For other cross-linked molecules with larger sized loops, separation of X-shaped molecules and looped molecules was observed.

For cross-link 4 (Figure 2), three reverse transcription stops at G791, A792, and U793 were seen (Figure 3F) whose partners were not identified by reverse transcription or by RNase H cleavage. U793 was already known to form the cross-link with A1518 by UV irradiation (*9*, T. Shapkina, personal communication), so the 3′ end of 16S rRNA was analyzed by the strategy where the cross-linked RNA was 3′-end-labeled and subjected to partial alkaline hydrolysis (*28*). The full-length 16S rRNA from fraction 4 did not give clear results in this experiment (results not shown), so a

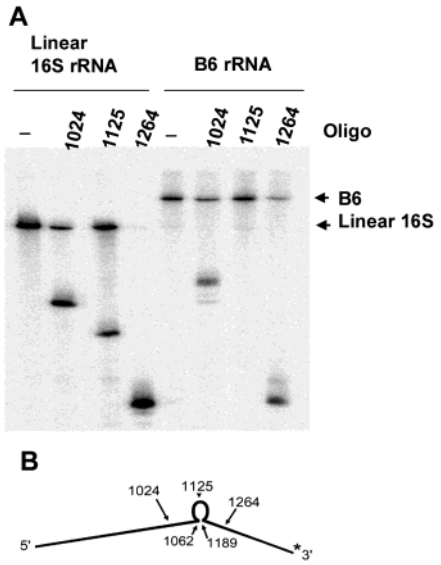

FIGURE 4: RNase H analysis of the cross-link U1189 × U1060−G1064. (A) Denaturing polyacrylamide gel electrophoresis of cross-link 6. RNA from band 6 from the preparative gel shown in Figure 2 was cleaved by RNase H. Lanes 1024, 1125, and 1264 represent the 3′-[^{32}P]-labeled linear 16S rRNA molecule and the 16S rRNA molecule containing the cross-link annealed to DNA oligonucleotides corresponding to the intervals 1016−1032, 1117−1133, and 1256−1273, respectively, and cleaved by RNase H. Lanes designated with "−" represent the uncut RNA from the linear 16S rRNA and the cross-linked B6 rRNA. The RNA was analyzed on a denaturing 3.6% polyacrylamide gel at a 19:1 ratio of acrylamide to bisacrylamide. The RNA fragment in lane 1024 from B6 rRNA had slower mobility than the RNA fragment in lane 1024 obtained from linear 16S rRNA. The RNA fragment in lane 1125 moved to a position similar to that of the uncut band in lane "−" in B6 rRNA. The fragments in lane 1264 from both linear 16S rRNA and B6 rRNA had similar mobility. (B) Cartoon of the B6 rRNA. The cleavage sites of the primers used are shown on the top of the cross-link, and the cross-linking sites are shown on the bottom of the panel.

preliminary oligonucleotide-directed RNase H cleavage in the interval 679−693 was done to allow a better isolation of the RNA containing cross-links in the 791−793 region. The truncated RNA (containing 679−1542) was purified by agarose gel electrophoresis and was 3′-[^{32}P]-end-labeled. The RNA was separated on 5% denaturing polyacrylamide gel electrophoresis at a 40:1 ratio of acrylamide to bisacrylamide (Figure 5A). All of the RNA fractions separated by gel electrophoresis were analyzed by reverse transcription (Figure 5B), and RNA from band 3 was found to produce the G791−U793 stops. Partial alkaline hydrolysis was carried out on the RNA from bands 3 and 2 and the linear RNA (all from the gel shown in Figure 5A), and the intensities of the resulting ladders were compared. An abrupt decrease in the intensities of the bands in the ladder was found to be at A1519, and therefore, it was assigned as the cross-linking site (Figure 5C,D). A similar strategy was used to determine which nucleotide of G791, A792, and U793 was involved in the cross-link with A1519. In this case, total cross-linked 16S rRNA was cleaved by RNase H at A759 using a mixed DNA/2′-OMe RNA oligonucleotide together with another DNA oligonucleotide in the interval 679−693 to break a contaminating cross-linked RNA molecule. The truncated RNA containing the fragment 759−1542 was agarose-gel-purified, 5′-[^{32}P]-labeled, and separated on a 5% polyacrylamide gel. Partial alkaline hydrolysis was used to determine U793 as the cross-linking partner for A1519 as described above (Figure 5E,F).

Re-irradiation experiments were done for isolated cross-linked 16S rRNA in TE buffer to determine if any of the cross-links were subject to photoreversal. None of the cross-links were found to reverse after irradiation at 330 or 254 nm for 5 or 10 min (data not shown). This is consistent with the structure that has been determined for s^{4}U−pyrimidine and s^{4}U−purine cross-links (*20*−*22*).

Determination of Cross-Linking Frequency. Cross-linking frequencies were obtained from the highly- or moderately-s^{4}U-substituted 16S rRNA (Figure 1B). The total cross-linking frequency was estimated to be ∼20% in the most highly substituted 16S rRNA and about 10% in the moderately substituted 16S rRNA. Cross-linking frequencies of the identified bands were calculated from the gel electrophoresis pattern and are listed in Table 1. The ratio of the frequencies of highly and moderately substituted RNA is approximately constant, indicating that there does not seem to be a detectable difference in the structure of the 30S subunits at different extents of s^{4}U substitution.

Identification of s^{4}U Substitutions in the 16S rRNA. s^{4}U substitution sites were found by reverse transcription after reaction of the s^{4}U-containing 16S rRNA with APAB. To improve detection of s^{4}U substitution sites, 16S rRNA with s^{4}U substitution was separated from nonthiolated RNA by electrophoresis on denaturing 3.6% APM−polyacrylamide (40:1 acrylamide/bisacrylamide) gel. The substituted RNA was purified from the gel slices by centrifugation in the presence of DTT (*31*) and was reacted with APAB. The APAB reaction was confirmed by re-electrophoresis of the 16S rRNA on an APM−PAGE gel (results not shown). The APAB-reacted s^{4}U-containing 16S rRNA was then analyzed by reverse transcription. It was expected that APAB reaction would interfere with reverse transcription, resulting in stops at positions one nucleotide before s^{4}U sites (Figure 2 in the Supporting Information). Eleven DNA primers were used to scan the 16S rRNA for s^{4}U substitution; all the reverse transcription stops are listed on the secondary structure of 16S rRNA (Figure 6).

DISCUSSION

The small number of cross-links observed here in the s^{4}U-substituted and irradiated 16S rRNA indicates a restricted pattern of cross-linking in the 30S subunit. When the same s^{4}U-containing 16S rRNA was irradiated after removal of proteins, a diffuse distribution of cross-linked molecules was seen in the gel electrophoresis assay indicative of a large number of low-frequency cross-links. In the 218-nucleotide RNA studied by the Favre group about 40 long-range cross-links were found (*18*), and if a proportional number of cross-links were formed in the whole 16S rRNA, several hundred different cross-links might be expected. There was already evidence that the organization of the 16S rRNA in the subunit reduces the number of different cross-links seen and raises the frequency of a few selected ones. The pattern of UVB-induced cross-links in the 30S subunit is significantly different in a buffer containing 0.5 mM Mg^{2+} compared to that found at 2 mM Mg^{2+} or greater (*9*), and it is known that changes in the [Mg^{2+}] in this range affect the overall compactness of the 30S subunit (*40*). In addition, cross-

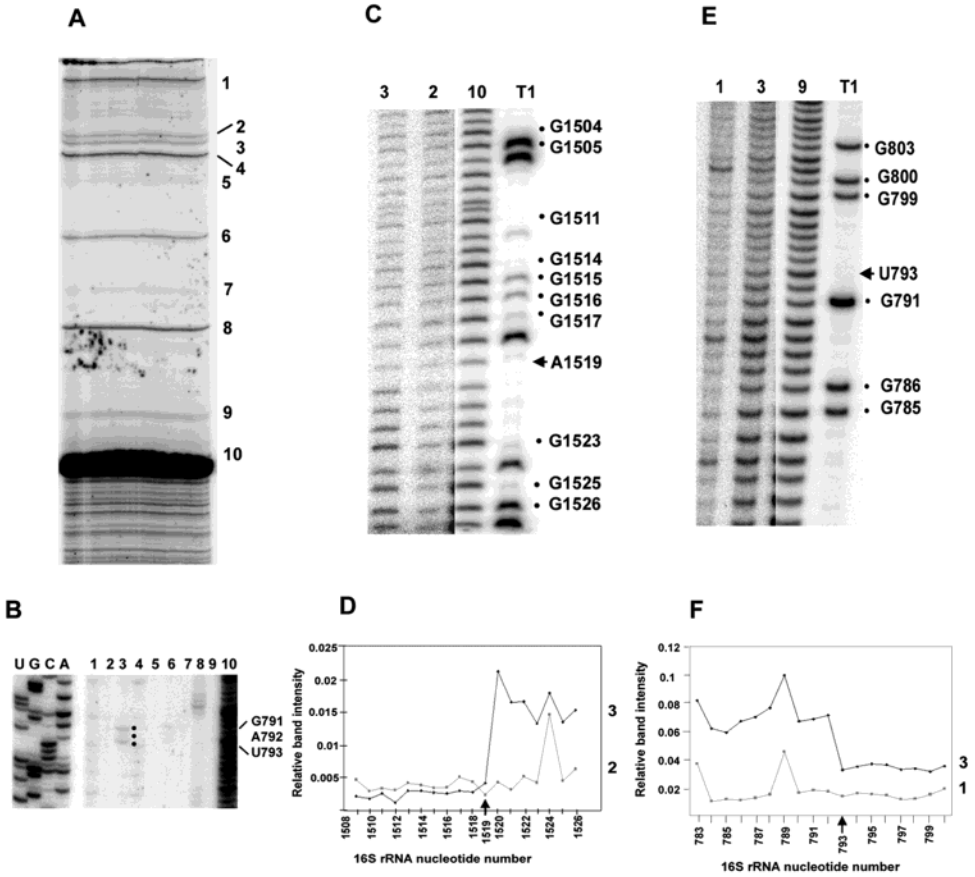

FIGURE 5: Identification of cross-linking partners for cross-link 4. Panels A−D show the identification of the A1519 cross-linked nucleotide. Panels E and F show the identification of the U793 cross-linked nucleotide. (A) Denaturing polyacrylamide gel electrophoresis of cross-linked molecules in 16S rRNA fragment 679−1542. RNA from irradiated 30S subunits was cleaved using a DNA oligonucleotide spanning the interval 679−693 and RNase H, and the 679−1542 fragment was agarose-gel-purified and 3′-end-labeled. RNA was separated on 5% denaturing polyacrylamide gel electrophoresis; fractions were numbered from 1 to 10. (B) Identification of the band containing the G791−U793 stops. Bands numbered 1−10 were subjected to reverse transcription through the interval 860−876, and RNA from band 3 produced reverse transcription stops at G791−U793. (C) Partial alkaline hydrolysis. RNA from bands 2 and 3 was subjected to alkaline hydrolysis. RNA from band 10 (linear RNA) was used as a control to determine the identity of the nucleotides in the ladder and G's in the T1 sequencing lane. The right side of the panel indicates the locations of G's and the arrow points to the position A1519 that is the first nucleotide of reduced intensity in the partial hydrolysis ladder in band 3. (D) Ratio of intensities after partial alkaline hydrolysis. Ratios of the intensity of each nucleotide in the ladder obtained from band 2 and band 3 to that obtained from the control lane 10 were plotted against all the nucleotides starting form the top of the gel toward the bottom of the gel. A drop in the ratio was observed at nucleotide A1519. (E) Partial alkaline hydrolysis. Cross-linked 16S rRNA fragment 759−1542 was isolated, 5′-end-labeled, and separated on a denaturing 5% polyacrylamide gel (not shown). RNA from bands 1 and 3 and linear RNA of the same fragment (band 9 in this experiment) were subjected to partial alkaline hydrolysis. RNA from band 9 (linear RNA) was used as a control to determine the locations of G's in the ladder. The right side of the panel indicates the locations of G's, and the arrow points to the position U793 that is the first nucleotide of reduced intensity in the partial hydrolysis ladder in band 3. (F) Ratio of intensities after partial alkaline hydrolysis. Ratios of the intensity of each nucleotide in the ladder obtained from band 1 and band 3 to that obtained from the control lane 9 were plotted against all the nucleotides starting form the bottom of the gel toward the top of the gel. A drop in the ratio was observed at nucleotide U793.

linking frequencies of site-specifically placed s^4U are quite high in reconstituted 30S subunits, but decrease by about 8-fold when those same 30S subunits are irradiated as reassociated 70S ribosomes (*19*). This indicates a further tightening of the reconstituted subunit structure when it is associated as a 70S ribosome.

The s^4U substitution sites and cross-link locations are shown in the 16S rRNA secondary structure diagram (Figure 6). The s^4U substitution sites are not random. This is likely not due to discrimination by RNA polymerase, but rather due to exclusion of 16S rRNA during the 30S assembly process because s^4U at some positions alters RNA−protein or RNA−RNA interactions or prevents inclusion of the 30S subunit in 70S ribosomes. s^4U cross-linking sites are shown in the 30S subunit atomic structure (Figure 7). The identities of the cross-linked nucleotides in nine regions separated by gel electrophoresis have been determined. These separated bands probably contain all of the most frequent long-range cross-links that are made within the 16S rRNA because the isolation of these molecules is based on the decreased electrophoretic mobility of the covalently looped RNA. Therefore, any frequent long-range cross-links should be included in this analysis. The gel conditions do not resolve loops smaller than 40 nucleotides in length, so short-range features were not determined. However, "linear" 16S rRNA after removal of the long-range cross-linked molecules was reverse transcribed nearly as completely as unirradiated control 16S rRNA, so it is unlikely that cross-links separated by less than 40 nucleotides are present at higher frequencies than the long-range cross-links. Three RNA fractions have been difficult to analyze. RNA from band 1 (Figure 2) had a number of reverse transcription stops, indicating that it

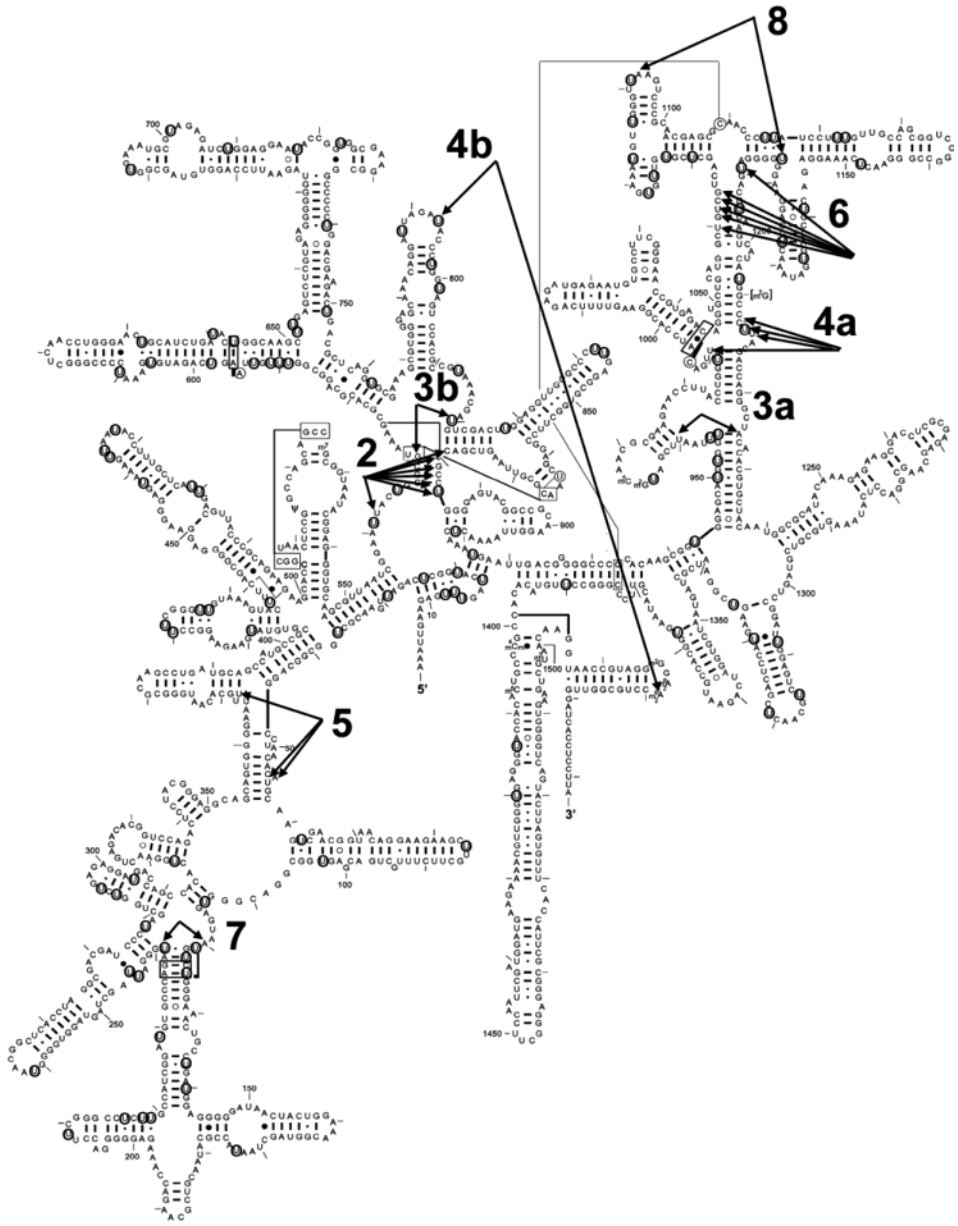

FIGURE 6: Identity of cross-links and locations of the s^4U substitutions in 16S rRNA. Cross-links are connected by the arrows and numbered according to Table 1. Circled nucleotides indicate uridines substituted by s^4U as determined by reverse transcription of the s^4U-containing 16S rRNA reacted with APAB. The 16S rRNA secondary structure is from Cannone et al. (*46*).

contains a mixture of cross-linked RNA species not resolved by the gel conditions used here. The total frequency of these is about half the frequency of the adjacent band 2. RNA from band 9 was not reverse transcribed by any of the 16S rRNA primers, suggesting that it contains 23S rRNA or a fragment of 23S rRNA that was not removed completely during agarose gel electrophoresis. Band 10 is probably due to a stable secondary structure in the 16S rRNA that is not completely melted under the electrophoresis conditions. Three other cross-links that appear at lower frequencies have not been identified because of the small amount of material obtained from the gels.

The majority of the cross-links are classified as the secondary structure type because they are in the vicinity of each other in the secondary structure (*41*). However, none occur within base-paired regions consistent with the suppression of s^4U cross-linking within secondary structures previously reported by Lemaigre-Dubreuil et al. (*18*). Five of the cross-links, U562 × C879−U884, U1183 × A1092, U793 × A1519, U991 × C1210−U1212, and U1189 × U1060−G1064, are similar to cross-links seen by UVB irradiation (see Table 1). In three of these examples (cross-link numbers 2, 4a, and 6), series of cross-linking sites include the cross-linking partners produced by UVB irradiation. In the other two examples (at cross-link numbers 4b and 8), the precise sites of cross-linking are shifted by one nucleotide, when the s^4U-induced and UVB-induced cross-linked pairs are compared. The remaining four cross-links, U960 × A1225, U820 × G570, U367 × U56−A55, and U239 × A120, do not have direct similarities to UVB-induced cross-links (*8*); however, even for these, all but U239 × A120 occur in the neighborhoods of UVB-induced cross-links. Thus, given the large number of possible cross-linking sites within the tertiary structure, there is a striking similarity between the places where s^4U−UVA-induced and UVB-induced cross-linking sites occur.

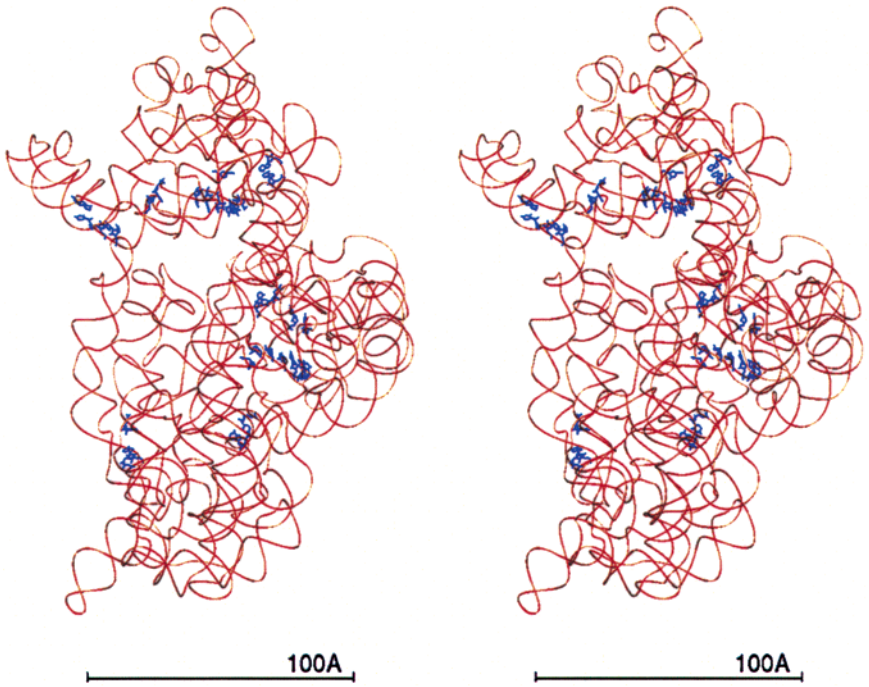

FIGURE 7: View of the s^{4}U cross-linked nucleotide pairs in the 16S rRNA structure, determined by Wimberly et al. (*2*). The orientation is a view with the 30S interface side facing the viewer. The 16S rRNA backbone is shown in orange ribbon with all the cross-linked nucleotides in blue.

At least 112 U positions were found as s^{4}U-substituted. However, this number must be an underestimate because several positions involved in cross-linking were not identified in the search for the s^{4}U-substituted sites. This could be due to incomplete APAB reaction at some positions or unequal s^{4}U substitution levels at different locations in the 16S rRNA. All of the cross-links identified involve a U residue as expected if s^{4}U is the agent responsible for their formation. However, factors other than the location of s^{4}U substitution must determine the cross-linking pattern. For instance, no s^{4}U substitution was detected at U367 or at U960, but these positions are involved in significant cross-linking. There are many other positions, on the other hand, which are relatively highly substituted but are not reactive in forming cross-links. Under the conditions used to obtain s^{4}U incorporation, about 60% of the 16S rRNA is without any incorporated s^{4}U judged by the behavior in gel electrophoresis on gels containing APM. Since the cells were grown for three generations after the switch to the s^{4}U/U mixture in the medium, there must be a significant amount of uridine in the cells that results in delay in the incorporation of s^{4}U into the RNA. The amount of s^{4}U substitution into the 30S subunit affects the frequency but not the pattern of cross-linking since the pattern is the same in RNA that is highly- versus moderately-s^{4}U-substituted.

The photochemistries for s^{4}U-induced and UVB-induced cross-linking are different as different parts of the nucleobases are involved in the cross-linking. s^{4}U forms stable covalent bonds with either pyrimidines or purines, and it is certain that s^{4}U−UVA photoreaction proceeds from an efficiently formed triplet state. The main photochemical pathway was identified as a (2 + 2) photoaddition of the excited C−S bond onto the 5,6 double bond of pyrimidines, yielding thietane intermediates, and their subsequent rearrangement in the dark to yield either 5−4 or 6−4 bipyrimidine photoadducts. A similar mechanism seems to be involved in the formation of photoadducts between 4-thiothymidine and adenosine, involving the C8/N7 double bond of adenosine. Importantly, the lifetime of the excited triplet state for s^{4}U is about 5 μs in different tRNA molecules where it occurs naturally (*42*, *43*). This is to be compared to the picosecond lifetime for the S_1 excited state and 0.35−1 μs for the T_1 excited state after UVB excitation (*44*, *45*). The many similarities between the positions of s^{4}U−UVA- and UVB-induced cross-linking seen here suggest that, despite the photochemistry differences, some other aspect of the ribosome structure allows nucleotide−nucleotide cross-link formation in certain regions. The very limited pattern of cross-link formation in the 30S ribosome subunit is in keeping with constraints placed on their formation probably through restrictions in conformational movements. On the other hand, in several instances s^{4}U cross-links occur at a series of contiguous nucleotides, and this does not occur with UVB-induced cross-linking. The most likely explanation is that in those particular sites the longer lifetime for s^{4}U excitation provides a longer time frame to obtain a suitable geometry for cross-linking, and this can occur at any of the possible partner nucleotides. s^{4}U−UVA-induced cross-links were not photoreversed at either 254 or 330 nm wavelength, which is not the case for UVB-induced cross-links. By virtue of not being photoreversed at the wavelength of irradiation, s^{4}U−UVA-induced cross-links should be better for monitoring changes in the structure of 30S ribosomal subunits as compared to UVB cross-links since the s^{4}U−UVA cross-linking frequencies are more indicative of their rate of formation.

Internucleotide distances between cross-linked partners have been measured in the 30S subunit crystal structure (*2*) (Table 1). Overall, there is a correlation in which the cross-linked nucleotide pairs that are closer in the X-ray structure tend to have higher cross-linking frequencies, indicating the relatedness of the X-ray structure and the 30S solution

structure. Six of the internucleotide distances for the s^4U-UVA cross-linked pairs are relatively short—between 3.3 and 6.2 Å. These distances are typical of the majority of UVB-induced cross-linked partners (*12*) and require relatively modest movements of the bases from their positions observed in the crystal structure to attain the van der Waals contact distance needed for covalent photoreaction. For the remaining 15 s^4U-UVA cross-linked pairs, the distances are between 11.4 and 21 Å, indicating that significantly larger distance displacements are needed for reaction. An important feature of these measurements is that the internucleotide distance distributions for s^4U-UVA and UVB cross-linked pairs are different, with a larger fraction of the s^4U-UVA nucleotide pairs at the larger distances. If cross-linking arose in those 30S subunits that have stable conformations that are slightly different from the equilibrium structure, there should not be this difference in the distance distributions in the two cross-linking methods. Therefore, it is more likely that the cross-links occur during RNA conformational fluctuations in the 30S subunit. The longer distance distribution for the s^4U-UVA cross-links again indicates that the longer excited-state lifetime for s^4U compared to UVB irradiation allows a larger number of opportunities for covalent reactions and even at larger departures from their equilibrium positions.

The base movements that are inferred by comparison of the cross-linking results and the X-ray structure must be specific ones and occur in only a limited region of the 30S subunit. Since s^4U is an intrinsic cross-linking agent, these displacements from the positions observed in the crystal structure reflect the movement of the nucleobases during the lifetime of the excited state. Whether there is a functional relevance for this is not clear yet. However, there is a clustering of cross-linking sites in the 30S subunit particularly in 16S rRNA domains III and II around the tRNA decoding region (Figure 7). The structural dynamics reflected in the cross-linking pattern may be involved in some way in tRNA binding or movement.

ACKNOWLEDGMENT

We thank Prof. Richard D'Ari for providing the *pyrD*$^-$ *E. coli* strain used in these experiments and Alain Expert-Bezancon for suggestions on the in vivo s^4U substitution method and extensive helpful comments on the manuscript. Tatjana Shapkina and Wayne Huggins are thanked for helpful discussions and providing internucleotide distance measurements.

SUPPORTING INFORMATION AVAILABLE

Two figures, one showing the separation of in vivo thiolated 16S rRNA on an APM−polyacrylamide gel to determine the distribution of the number of s^4U's in the RNA and one showing two examples of reverse transcription analyses of APAB-modified s^4U-containing 16S rRNA to determine the locations of the s^4U sites. This material is available free of charge via the Internet at http://pubs.acs.org.

REFERENCES

1. Cate, J. H., Yusupov, M. M., Yusupova, G. Z., Earnest, T. N., and Noller, H. F. (1999) X-ray crystal structures of 70S ribosome functional complexes, *Science 285*, 2095−2104.
2. Wimberly, B. T., Brodersen, D. E., Clemons, W. M., Morgan-Warren, R. J., Carter, A. P., Vonrhein, C., Hartsch, T., and Ramakrishnan, V. (2000) Structure of the 30S ribosomal subunit, *Nature 407*, 327−339.
3. Schluenzen, F., Tocilj, A., Zarivach, R., Harms, J., Gluehmann, M., Janell, D., Bashan, A., Bartels, H., Agmon, I., Franseschi, F., and Yonath, A. (2000) Structure of functionally activated small ribosomal subunit at 3.3 A resolution, *Cell 102*, 615−623.
4. Ban, N., Nissen, P., Hansen, J., Moore, P. B., and Steitz, T. A. (2000) The complete structure of the large ribosomal subunit at 2.4 Å resolution, *Science 289*, 905−920.
5. Yusupov, M. M., Yusupova, G. Z., Baucom, A., Lieberman, K., Earnest, T. N., Cate, J. H., and Noller, H. F. (2001) Crystal structure of the ribosome at 5.5 Å resolution, *Science 292*, 883−896.
6. Agarwal, R. K., Latta, R. K., and Frank, J. (1999) Conformational variability in *Escherichia coli* 70S ribosome as revealed by 3-D cryo-electron microscopy, *Int. J. Biochem. Cell Biol. 31*, 243−254.
7. Frank, J. (2003) Electron microscopy of functional ribosome complexes, *Biopolymers 68*, 223−233.
8. Wilms, C., Noah, J. W., Zhong, D., and Wollenzien, P. (1997) Exact determination of UV-induced crosslinks in 16S ribosomal RNA in 30S ribosomal subunits, *RNA 3*, 602−612.
9. Noah, J. W., and Wollenzien, P. (1998) Dependence of the 16S rRNA decoding region structure on Mg^{2+}, subunit association and temperature, *Biochemistry 37*, 15442−15448.
10. Shapkina, T. G., Dolan, M. A., Babin, P., and Wollenzien, P. (2000) Initiation factor 3 induced structural changes in the 30S ribosomal subunit and in complexes containing $tRNA^{fMet}$ and mRNA, *J. Mol. Biol. 299*, 617−630.
11. Noah, J. W., Shapkina, T. G., Nanda, K., Huggins, W., and Wollenzien, P. (2003) Conformational change in the 16S rRNA in the *Escherichia coli* 70S ribosome induced by P/P- and P/E-site $tRNA^{Phe}$ binding, *Biochemistry 42*, 14386-14396.
12. Shapkina, T., Lappi, S., Franzen, S., and Wollenzien, P. (2004) Efficiency and pattern of UV pulse laser induced RNA-RNA crosslinking in the ribosome, *Nucleic Acids Res. 32*, 1518−1526.
13. Favre, A. (1990) 4-Thiouridine as an intrinsic photoaffinity probe of nucleic acid structure and interactions, in *Bioorganic Photochemistry: Photochemistry and the nucleic acids* (Morrison, H., Ed.) pp 379−425, Wiley, New York.
14. Hajnsdorf, E., Favre, A., and Expert-Bezancon, A. (1986) Multiple crosslinks of proteins S7, S9, S13 to domains 3 and 4 of 16S RNA in the 30S particle, *Nucleic Acids Res. 10*, 4009−4022.
15. Hajnsdorf, E., Lemaigre-Dubreuil, Y., Bezerra, R., Y., Favre, A., and Expert-Bezancon, A. (1987) RNA protein crosslinks introduced into *E. coli* ribosomes by use of the intrinsic probe 4-thiouridine, *Photochem. Photobiol. 45* (4), 445−451.
16. Hajnsdorf, E., Favre, A., and Expert-Bezancon, A. (1989) New RNA-protein crosslinks in domain 1 and 2 of *E. coli* 30S ribosomal subunits obtained by means of an intrinsic photoaffinity probe, *Nucleic Acids Res. 17*, 1475−1491.
17. Kumar, R. K., and Davis, D. R. (1997) Synthesis and studies on the effects of 2-thiouridine and 4-thiouridine on sugar conformation and RNA duplex stability, *Nucleic Acids Res. 25*, 1272−1280.
18. Lemaigre-Dubreuil, Y., Expert-Bezancon, A., and Favre, A. (1991) Conformation and structural fluctuations of a 218 nucleotides long rRNA fragment: 4-thiouridine as an intrinsic photolabelling probe, *Nucleic Acids Res. 19*, 3653−3660.
19. Juzumiene, D., and Wollenzien, P. (2001) Arrangement of the central pseudoknot region of 16S rRNA in the 30S ribosomal subunit determined by site-directed 4-thiouridine crosslinking, *RNA 7*, 71−84.
20. Leonard, N. J., Bergstrom, D. E., and Tolman, G. L. (1971) Intramolecular cross-linking of single stranded copolymers of 4-thiouridine and cytidine, *Biochem. Biophys. Res. Commun. 44*, 1524−1530.
21. Bergstrom, D. E., and Leonard, N. J. (1972) Photoreaction of 4-thiouracil with cytosine. Relation to photoreactions in *Escherichia coli* transfer ribonucleic acids, *Biochemistry 11*, 1−9.
22. Saintome, C., Clivio, P., Favre, A., Fourrey, J. L., and Riche, C. (1996) RNA photolabeling mechanistic studies: X-ray crystal structure of the photoproduct formed between 4-thiothymidine and adenosine upon near UV irradiation, *J. Am. Chem. Soc. 118*, 8142−8143.
23. Favre, A., Bezerra, R., Hajnsdorf, E., Lemaigre Dubreuil, Y., and Expert-Bezancon, A. (1986) Substitution of uridine in vivo by the intrinsic photoactivable probe 4-thiouridine in *Escherichia coli* RNA, *Eur. J. Biochem. 160*, 441−449.

24. Bezerra, R., and Favre, A. (1990) *In vivo* incorporation of the intrinsic photolabel 4-thiouridine into *Escherichia coli* RNA, *Biochem. Biophys. Res. Commun. 166*, 29−37.
25. Miller, J. H. (1972) *Experiments in molecular genetics*, Cold Spring Harbor Laboratory, Cold Spring Harbor, NY.
26. Makhno, V. I., Peshin, N. N., Semenkov, Y. P., and Kirillov, S. V. (1988) Modified method of producing "tight" 70S ribosomes from *Escherichia coli*, highly active in individual stages of the elongation cycle, *Mol. Biol.* 22, 528−537.
27. Isaacs, S. T., Shen, C.-K. J., Hearst, J. E., and Rapoport, H. (1977) Synthesis and characterization of new psoralen derivatives with superior photoreactivity with DNA and RNA, *Biochemistry 16*, 1058−1064.
28. Juzumiene, D., Shapkina, T., Kirillov, S., and Wollenzien, P. (2001) Short-range RNA-RNA crosslinking methods to determine rRNA structure and interactions, *Methods 25*, 333−343.
29. Wilms, C., and Wollenzien, P. (1994) Purification of RNA from polyacrylamide gels by ultracentrfugation, *Anal. Biochem. 221*, 204−205.
30. Inoue, H., Hayase, Y., Iwai, S., and Ohtsuka, E. (1987) Sequence-dependent hydrolysis of RNA using modified oligonucleotide splints and RNase H, *FEBS Lett. 215*, 327−330.
31. Igloi, G. (1988) Interaction of tRNAs and of phosphorothioate-substituted nucleic acids with an organomercurial. Probing the chemical environment of thiolated residues by affinity electrophoresis, *Biochemistry 27*, 3842−3849.
32. Stade, K., Rinke-Appel, J., and Brimacombe, R. (1989) Site-directed cross-linking of mRNA analogues to the *Escherichia coli* ribosome; identification of 30S ribosomal components that can be cross-linked to the mRNA at various points 5′ with respect to the decoding site, *Nucleic Acids Res. 17* (23), 9889−9908.
33. Moazed, D., and Noller, H. F. (1986) Transfer RNA shields specific nucleotides in 16S ribosomal RNA from attack by chemical probes, *Cell 47*, 985−994.
34. Ericson, G., Minchew, P., and Wollenzien, P. (1995) Structural changes in base-paired region 28 in 16S rRNA close to the decoding region of the 30S ribosomal subunit are correlated to changes in tRNA binding, *J. Mol. Biol. 250*, 407−419.
35. Moazed, D., and Noller, H. F. (1990) Binding of tRNA to the ribosomal A and P sites protects two distinct sets of nucleotides in 16S rRNA, *J. Mol. Biol. 211*, 135−145.
36. Montpetit, A., Payant, C., Nolan, J. M., and Brakier-Gingras, L. (1998) Analysis of the conformation of the 3′ major domain of Escherichia coli 16S ribosomal RNA using site-directed photoaffinity crosslinking, *RNA 4*, 1455−1466.
37. Denman, R., Negre, D., Cunningham, P. R., Nurse, K., Colgan, J., Weitzmann, C., and Ofengand, J. (1989) Effect of point mutations in the decoding site (C1400) region of 16S ribosomal RNA on the ability of ribosomes to carry out individual steps of protein synthesis, *Biochemistry 28*, 1012−1019.
38. Cunningham, P. R., Nurse, K., Bakin, A., Weitzmann, C. J., Pflumm, M., and Ofengand, J. (1992) Interaction between two conserved single-stranded regions at the decoding site of small subunit ribosomal RNA is essential for ribosome function, *Biochemistry 31*, 12012−12022.
39. Ericson, G., and Wollenzien, P. (1988) Use of reverse transcription to determine the exact locations of psoralen photochemical crosslinks in RNA, *Anal. Biochem. 174*, 215−223.
40. Moazed, D., Van Stolk, B. J., Douthwaite, S., and Noller, H. F. (1986) Interconversion of active and inactive 30S ribosomal subunits is accompanied by a conforamtional changes in the decoding region of 16S rRNA, *J. Mol. Biol. 191*, 483−493.
41. Zweib, C., and Brimacombe, R. (1980) Localization of series of intra-RNA cross-links in 16S RNA, induced by ultraviolet irradiation of *Escherichia coli* 30S ribosomal subunits, *Nucleic Acids Res. 8*, 2397−2411.
42. Shalitin, N., and Feitelson, J. (1976) 4-Thiouridine, a built-in probe for structural changes in transfer RNA, *Biochemistry 15*, 2092−2097.
43. Milder S. J., Weiss P. S., and Kliger, D. S. (1989) Time-resolved absorption, circular dichroism, and emission of tRNA. Evidence that the photo-cross-linking of 4-thiouridine in tRNA occurs from the triplet state, *Biochemistry 28*, 2258−2264.
44. Budowsky E. I., Axentyeva M. S., Abdurashidova G. G., Simukova N. A., and Rubin L. B. (1986) Induction of polynucleotide-protein cross-linkages by ultraviolet irradiation: Pecularities of the high-intensity laser pulse irradiation, *Eur. J. Biochem. 159*, 95−101.
45. Salet C., and Bensasson R. (1975) Studies on thymine and uracil triplet excited state in acetonitrile and water, *Photochem. Photobiol. 22*, 231−235.
46. Cannone, J., Subramanian, S., Schnare, M., Collett, J., S'Souza, L., Du, Y., Feng, B., Lin, N., Madabusi, L., Muller, K., Pande, N., Shang, Z., and Gutell, R. (2002) The comparative RNA Web (CRW) site: an online database of comparative sequence and structure information for ribosomal, intron and other RNAs, *Biomed. Cent. Bioinf. 3*, 2.
47. Stiege, W., Kosack, M., Stade, K., and Brimacombe, R. (1988) Intra-RNA cross-linking in *Escherichia coli* 30S ribosomal subunits: Selective isolation of cross-linked products by hybridization to specific cDNA fragments, *Nucleic Acids Res. 16*, 4315−4329.

BI049702H